Y. Sudo
Head, Division of HTTR Project Management,
Oarai Research Establishment,
Japan Atomic Energy
Research Institute (JAERI),
Oarai-machi, Higashiibaraki-gun,
Ibaraki-ken, 311-13 Japan

M. Kaminaga
Research Engineer,
Research Reactor Technology
Development Division,
Department of Research Reactor,
Tokai Research Establishment,
Japan Atomic Energy
Research Institute (JAERI),
2-4 Shirakata-Shirane, Tokai-mura,
Naka-gun, Ibaraki-ken, 319-11 Japan

A New CHF Correlation Scheme Proposed for Vertical Rectangular Channels Heated From Both Sides in Nuclear Research Reactors

In this study, an investigation was carried out to identify the important parameters affecting critical heat flux (CHF) in rectangular channels, focusing on the effects of flow direction, channel inlet subcooling from 1 to 213 K, the channel outlet condition extending from subcooling of 0–74 K to quality of 0–1.0, pressure of 0.1 to 4 MPa, water mass flux of −25,800 to +6250 kg/m²s, and channel configuration. In particular, the effect of the outlet subcooling in upflow and downflow on the CHF was quantitatively investigated. As a result of this study, a new CHF scheme covering downflow, countercurrent flow, and upflow was established in the rectangular channels within the ranges of parameters investigated in this study.

Introduction

The quantitative understanding of critical heat flux (CHF) for vertical rectangular channels is essential and required for core thermohydraulic design and safety analysis of nuclear research reactors in which flat-plate-type fuel is employed. In the safety design, some abnormal operational occurrences and accidents have been assumed. In the case of a pool-type nuclear research reactor in which steady-state core flow is downward, a transient core flow is considered in which the flow rate decreases from a steady-state downward flow to a zero flow, and then an upward flow is established as a cooling mode of natural convection to remove the decay heat after a reactor scram in case of abnormal operational occurrences and accidents. A detailed understanding of CHF is, accordingly, essential not only for a downward flow but also for an upward flow, including a flow subject to flooding conditions, that is, a countercurrent flow, in order to assure the intactness of fuel under normal operations, abnormal operational occurrences, and accidents. It should be noted that when the coolant flow rate decreases to zero and the flow becomes stagnant, the flow would become a countercurrent flow with downward water flow and upward flow of bubbles or steam generated in the channel. This is a flooding condition, because the flow channels are submerged in a water pool in the nuclear research reactor.

Many existing nuclear research reactors are approaching the end of their lifetime. Nuclear research reactors that are to be reconstructed or planned in the near future will be designed to have a higher neutron flux and a higher power density than ever. Therefore, to remove heat generated in the core, coolant mass flux will be very high and the coolant will be pressurized. Under such conditions, the channel outlet coolant would be subcooled not only for normal operation but also in abnormal occurrences.

The existing correlations and schemes for predicting CHF in the rectangular channels were investigated by the authors from the point of view of their applicability to the core thermohydraulic design and safety analysis. It was found that differences in CHF between an upward flow and a downward flow under the subcooled condition at the channel outlet, i.e., at a rather high mass flux region, have not been fully clarified systematically for vertical rectangular channels heated from both sides or from one side.

Therefore, in this study, the effect of dominant factors on CHF was investigated based on the existing CHF experimental data to establish a CHF scheme that is applicable for nuclear research reactors using flat-plate-type fuel. A new correlation scheme was proposed as the results of this investigation.

Previous CHF Correlation Scheme for Rectangular Channels

A CHF correlation scheme for rectangular channels previously proposed by the authors consists of three CHF correlations (Sudo et al., 1985a), which were used for the core thermohydraulic design and safety analysis of the upgraded JRR-3 (Sudo et al., 1985b; Hirano and Sudo, 1986).

The authors' CHF correlation scheme is illustrated in Fig. 1. The correlations used in the scheme are shown as follows:

$$q^*_{CHF,1} = 0.005 \cdot |G^*|^{0.611} \tag{1}$$

for both upflow ($G^* > G^*_2$) and downflow ($G^* > G^*_1$),

$$q^*_{CHF,2} = \frac{A}{A_H} \cdot \Delta T^*_{SUB,in} \cdot |G^*| \tag{2}$$

for downflow in the region where $q^*_{CHF,2} \le q^*_{CHF,1}$, that is, $G^* \le G^*_1$, and

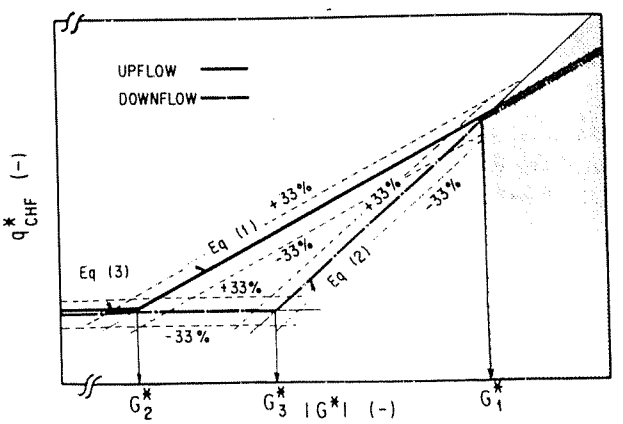

Fig. 1 Previous CHF correlation scheme proposed by authors for rectangular channels for $\Delta T^*_{SUB,0} = 0$

Contributed by the Heat Transfer Division and presented at the 1st JSME-ASME Joint International Conference on Nuclear Engineering, Tokyo, Japan, November 5-7, 1991. Manuscript received by the Heat Transfer Division January 1992; revision received December 1992. Keywords: Boiling, Forced Convection, Multiphase Flows. Associate Technical Editor: L. C. Witte.

$$q^*_{CHF,3} = 0.7 \frac{A}{A_H} \cdot \frac{\sqrt{W/\lambda}}{\{1+(\rho_g/\rho_l)^{1/4}\}^2} \quad (3)$$

as the minimum CHF for both upflow ($G^* \le G^*_2$) and downflow ($G^* \le G^*_3$), where G^*_1 is given by $q^*_{CHF,1} = q^*_{CHF,2}$, G^*_2 by $q^*_{CHF,1} = q^*_{CHF,3}$, and G^*_3 by $q^*_{CHF,2} = q^*_{CHF,3}$, respectively; and

$$G^* = \frac{G}{\sqrt{\lambda g \rho_g (\rho_l - \rho_g)}},$$

$$q^*_{CHF} = \frac{q_{CHF}}{h_{fg}\sqrt{\lambda g \rho_g (\rho_l - \rho_g)}}.$$

It should be pointed out here that Eq. (2) gives the condition that the outlet subcooling equals zero, that is, $\Delta T^*_{SUB,0} = 0$.

Equation (1) is a correlation proposed by Sudo et al. (1985a). Equations (2) and (3) are correlations proposed originally by Mishima (1984; Mishima et al., 1983). Mishima could not make clear the applicability of these correlations fully enough because of small number of available experimental data. The authors accumulated the available experimental data, carrying out the experiments with rectangular channels. They have shown that the correlation error of the CHF scheme is within 33 percent of rms error against the experimental data. It was found that the scheme is applicable for the region of $0 \le |G^*| < 3000$.

According to the results previously investigated by the authors (Sudo et al., 1985a), it was concluded that the CHF for upflow in the region of $q^*_{CHF,1} \ge q^*_{CHF,2}$ was expressed by Eq. (1) and the CHF for downflow in the region of $q^*_{CHF,1} \ge q^*_{CHF,2}$ was expressed by Eq. (2). For both upflow and downflow, there is a minimum CHF, which is defined by Eq. (3). On the other hand, the CHF for both upflow and downflow in the region of $q^*_{CHF,1} \le q^*_{CHF,2}$, which is shown as a shaded region in Fig. 1, was expressed by Eq. (1). In the shaded region, a channel outlet coolant condition is a subcooled one with a very high coolant mass flux $|G^*|$. An effect of channel outlet subcooling $\Delta T_{SUB,0}$ on the CHF was not considered in Eq. (1) in the CHF scheme described above because such a highly subcooled condition at the outlet was not expected in the core thermohydraulic design and safety analysis of the upgraded JRR-3 where the outlet subcooling is in the range of 0 to 20 K.

Other typical existing correlations considered to be applicable to the rectangular channels would be those proposed by Katto (1981), Mirshak et al. (1959), Zenkevich (1959), and Gambill and Bundy (1961).

Katto proposed the following correlations for the CHF in the rectangular channels through comparison between the previous experimental data of Yücel and Kakac (1978), Gambill and Bundy (1961), and others and the correlations he originally proposed for round and annular tubes.

Katto's correlations are expressed as follows for low mass flux, medium mass flux, and high mass flux, respectively:

$$q^*_{CHF,41} = 0.25\left(\frac{Dh}{L}\right)(1+\Delta T^*_{SUB,in})G^* \quad (4)$$

for low mass flux,

$$q^*_{CHF,42} = \left\{0.25+0.0009\left(\frac{L}{Dh}-50\right)\right\}\left(\frac{Dh}{L}\right)\left\{\frac{1}{L}\left(\frac{\sigma}{\rho_l g}\right)^{1/2}\left(\frac{\rho_l}{\rho_g}\right)\frac{1}{G^{*2}}\right\}^{0.043} \cdot \left[1+\frac{1.043\Delta T^*_{SUB,in}}{4\left\{0.25+0.0009\left(\frac{L}{Dh}-50\right)\right\}\left\{\frac{1}{L}\left(\frac{\sigma}{\rho_l g}\right)^{1/2}\left(\frac{\rho_l}{\rho_g}\right)\frac{1}{G^{*2}}\right\}^{0.043}}\right]G^* \quad (5)$$

for medium mass flux, and

$$q^*_{CHF,43} = 0.15\left(\frac{\rho_l}{\rho_g}\right)^{0.133}\frac{\left\{\frac{1}{L}\left(\frac{\sigma}{\rho_g g}\right)^{1/2}\left(\frac{\rho_l}{\rho_g}\right)^{1/2}\frac{1}{G^{*2}}\right\}^{1/3}}{1+0.0077\frac{L}{Dh}} \cdot \left[1+\frac{5}{9}\frac{\left(0.0308+\frac{Dh}{L}\right)\cdot\Delta T^*_{SUB,in}}{\left\{\frac{1}{L}\left(\frac{\sigma}{\rho_g g}\right)^{1/2}\left(\frac{\rho_l}{\rho_g}\right)^{1/2}\frac{1}{G^{*2}}\right\}^{1/3}\left(\frac{\rho_g}{\rho_l}\right)^{0.133}}\right]G^* \quad (6)$$

for high mass flux.

Here, the low mass flux region is defined for G^* of $q^*_{CHF,41} \le q^*_{CHF,42}$, the medium mass flux region for G^* of $q^*_{CHF,42} \le$

Nomenclature

A = flow area of channel, m^2
A_H = heated area of channel, m^2
Cp = specific heat of liquid, J/(kg•K)
De = equivalent hydraulic diameter, m
Dh = equivalent heated diameter, m
g = acceleration of gravity, m/s^2
G = mass flux, $kg/m^2 \cdot s$
G^* = dimensionless mass flux
G^*_1 = boundary value of G^* given by $q^*_{CHF,1} = q^*_{CHF,2}$
G^*_2 = boundary value of G^* given by $q^*_{CHF,1} = q^*_{CHF,3}$
G^*_3 = boundary value of G^* given by $q^*_{CHF,2} = q^*_{CHF,3}$
h = heat transfer coefficient, kW/m^2K
h^* = dimensionless heat transfer coefficient = $h/Cp\sqrt{\lambda \rho_g g(\rho_l - \rho_g)}$
h_{fg} = latent heat of evaporation, J/kg
L = length of channel, m
P = pressure, MPa
q = heat flux, kW/m^2
q^* = dimensionless heat flux
$q^*_{CHF,1}$ = defined by Eq. (1)
$q^*_{CHF,2}$ = defined by Eq. (2)
$q^*_{CHF,3}$ = defined by Eq. (3)
T = temperature, K
T^* = dimensionless temperature = $Cp \cdot T/h_{fg}$
W = width of channel, m
ΔT_s = superheat = $T_w - T_s$, K
ΔT^*_s = dimensionless superheat = $Cp(T_w - T_s)/h_{fg}$, K
ΔT_{SUB} = subcooling, K
ΔT^*_{SUB} = dimensionless subcooling = $Cp \cdot \Delta T_{SUB}/h_{fg}$
λ = characteristic length = $[\sigma/(\rho_l - \rho_g) \cdot g]^{1/2}$, m
ν = kinematic viscosity, m^2/s
ρ = density, kg/m^3
σ = surface tension, N/m

Subscripts

b = bulk
CHF = critical heat flux
g = vapor
in = inlet
l = liquid
o = outlet
s = saturation
w = heated surface

$q^*_{CHF,43}$, and the high mass flux region for G^* of $q^*_{CHF,42} > q^*_{CHF,43}$, respectively.

The effects of pressure, mass flux, subcooling, and the ratio of channel length to heated equivalent diameter were taken into account as key parameters in the above correlations. As the number of available experimental data was small, as stated in his article, only the availability of Eq. (5) could be investigated for high mass flux. He noticed that the magnitude of CHF in downflow obtained by Gambill and Bundy (1961) were clearly smaller than that in upflow obtained previously but the number of available existing data was so small that he could not investigate the difference in CHF characteristics between upflow and downflow. A feature of Katto's correlations is that the CHF approaches zero as the G^* approaches zero.

Mirshak et al. (1959) proposed for downflow the following correlation in which the effects of water velocity, subcooling, and pressure were taken into account as key parameters, based on the experiments for downflow with a medium mass flux of 500 to 1300 kg/m^{2}s and outlet subcooling of 6 to 74 K:

$$q^*_{CHF} = 360 \cdot \frac{1+0.129G^*\left\{\lambda\left(\frac{\rho_g}{\rho_l}\right)\left(1-\frac{\rho_g}{\rho_l}\right)g\right\}^{1/2}}{h_{fg}\cdot\{\lambda\rho_g(\rho_l-\rho_g)g\}^{1/2}} \cdot\left\{1+0.009\left(\frac{h_{fg}}{Cp}\right)\Delta T^*_{SUB,0}\right\}(1+1.86P) \quad (7)$$

A feature of the correlation proposed by Mirshak et al. is that CHF approaches a constant, which is not zero and is determined by pressure and subcooling, as shown below, when G^* approaches zero:

$$q^*_{CHF} = \frac{360\left\{1+0.009\left(\frac{h_{fg}}{Cp}\right)\Delta T^*_{SUB,0}\right\}(1+1.86P)}{h_{fg}\{\lambda\cdot\rho_g(\rho_l-\rho_g)g\}^{1/2}} \quad (8)$$

Zenkevich (1959) proposed for upflow the following correlation, in which the effect of pressure, subcooling, and mass flux were taken into account:

$$q^*_{CHF} = \frac{2.5\times10^{-5}\left(\frac{\sigma}{\nu_l}\right)^{1/2}}{\{\lambda\rho_g(\rho_l-\rho_g)g\}^{1/4}}(1+73.6\cdot\Delta T^*_{SUB,0})\cdot G^{*1/2} \quad (9)$$

A feature of Eq. (9) is that CHF is proportional to $G^{*1/2}$, and then approaches zero as G^* approaches zero.

Gambill and Bundy (1961) proposed a correlation with a form shown below for a subcooled forced-convection flow in a vertical rectangular channel.

$$q^*_{CHF} = 0.18\cdot\left\{1+\frac{1}{9.8}\left(\frac{\rho_l}{\rho_g}\right)^{3/4}\Delta T^*_{SUB}\right\} + h^*(\Delta T^*_s + \Delta T^*_{SUB}) \quad (10)$$

Here, ΔT^*_s is given by a correlation that is determined with the saturation temperature T_s and the critical heat flux, and h^* is given by a heat transfer correlation for a single-phase turbulent forced convection flow. A feature of Eq. (10) is that q^*_{CHF} does not approach zero with decreasing G^*, but approaches a constant given by $q^*_{CHF} = 0.18$ with G^* approaching zero under saturated conditions.

In Fig. 2, for comparison, Eqs. (1), (3), (4), (5), (6), (9), and (10) are illustrated for upflow with the conditions of P = 0.11 MPa, $\Delta T^*_{SUB,in} = 0$ and $\Delta T^*_{SUB,0} = 0$ along with the typical experimental data whose $\Delta T^*_{SUB,0}$ is less than 4 K. Here, Eqs. (3), (4), (5), (6), and (10) are illustrated for a rectangular channel heated from both sides (L = 0.75 m, W = 0.05 m, and gap = 2.25 mm), which were investigated by Sudo et al. (1985a). These equations include the effects of channel configuration. Zenkevich's correlation gives overly conservative predictions for the experimental data for high mass flux. On the other hand, Katto's correlation for low mass flux gives overly conservative predictions to the experimental data. The correlation given by Eq. (1) shows a good prediction for the experimental data whose $\Delta T^*_{SUB,0}$ is almost zero.

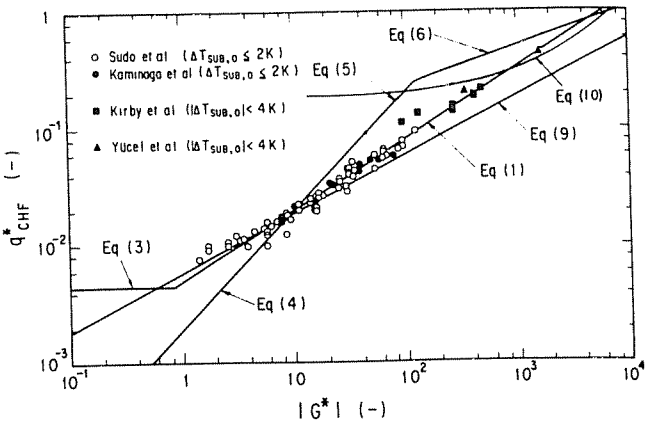

Fig. 2 Comparison of typical previous CHF correlations ($\Delta T^*_{SUB,0}$ = 0) with experimental data for upflow (Kaminaga et al., 1991; Kirby et al., 1967; Sudo et al., 1985a; Yücel and Kakac, 1978)

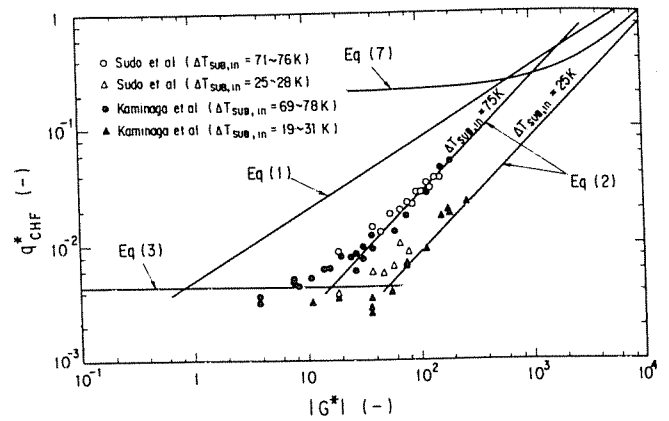

Fig. 3 Comparison of typical previous CHF correlations with experimental data for downflow (Kaminaga et al., 1991; Sudo et al., 1985a)

Equation (1) is also illustrated in Fig. 3 so as to make clear the differences in CHF characteristics between upflow and downflow. Equations (2) and (3) show a good prediction for the experimental data of downflow for the low and medium mass fluxes of $G^* \le G^*_1$.

From the discussion described above, it is very clear for $G^* \le G^*_1$ that Eq. (1) would be a proper correlation for predicting the experimental data of $\Delta T^*_{SUB,0} = 0$ for upflow, and Eqs. (2) and (3) for downflow. However, the effect of subcooling, $\Delta T^*_{SUB,0}$, is not clear on the CHF for $G^* \ge G^*_1$, although the effect should be properly taken into account in Eq. (1) for both upflow and downflow so that the thermohydraulic design and safety analysis may be reasonably done without giving overly conservative results for $G^* \ge G^*_1$.

Effects of Channel Outlet Subcooling ($\Delta T_{SUB,0}$)

In this study, Eq. (1) was selected as a base correlation to

Table 1 Test conditions of existing tests investigated in this study

Author(s)	Pressure (MPa)	Mass flux (kg/m^{2}s)	Inlet water subcooling (K)	Outlet condition subcooling (K)	Outlet condition quality (-)	CHF (kW/m^2)	L/De (-)	A/A$_H$ (-)	Number of data(-)
Sudo et al. (1985a)*	0.1~0.12 (Inlet)	-600~+480	20~81	0.0~27	0.0~1.0	32~320	170	1.88×10^{-3}	40[U,D]*1)
						66~830	71	4.67×10^{-3}	37[U,D]
Kaminaga, et al. (1991)*	0.1~0.12 (Inlet)	-2,200~+450	2.3~78	0.0~33	0.0~1.0	22~1,190	170	1.88×10^{-3}	203[U,D]
	0.1 (Inlet)	-340~+330	1.3~75	0.0~24	0.0~1.0	54~540	83	4.17×10^{-3}	63[U,D]
Yücel and Kakac (1978)**	0.1 (Inlet)	-6,250~+6,250	3.2~44	0.0~37	0.0~0.01	1,580~5,820	40	3.35×10^{-2}	16[U,D]
Kirby et al. (1967)***	0.18 (Inlet)	-2,720~+2,720	2.9~46	0.6~43	-	1,170~5,810	8	1.65×10^{-1}	49[U,D]
Mirshak et al. (1959)**	0.17~0.6 (Outlet)	-12,500~-5,030	27~104	6.0~74	-	3,980~10,000	41	8.51×10^{-3}	51[D]
							~77	1.65×10^{-2}	
Gambill and Bundy (1961)**	1.1~4.0 (Outlet)	-25,800~-9,210	151~213	14~55	-	8,270~19,400	128	1.18×10^{-3}	10[D]
							~240	-2.20×10^{-3}	
Mishima (1984)*,**	0.1 (Inlet)	-610~+360	13~71	0.0~21	0.0~1.0	56~1,170	77	4.57×10^{-3}	51[U,D]
								-9.14×10^{-3}	58[U,D]
Komori et al. (1990)*	0.1~0.72 (Inlet)	-2,440~-610	51~117	0.0~12	0.0~0.03	322~1,630	150	2.93×10^{-3}	18[D]

* Rectangular channel, Heated from both sides. ** Rectangular channel, Heated from one side.
*** Rectangular channel, Heated by round tube. *1) U : Upflow, D : Downflow

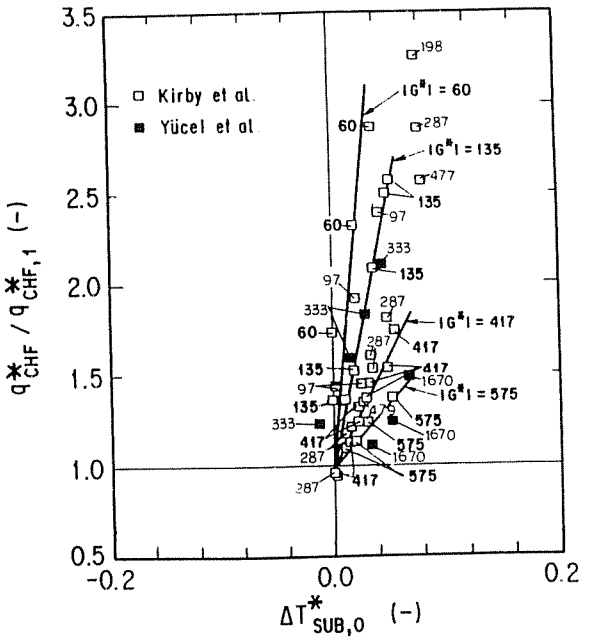

Fig. 4 Effects of $\Delta T^*_{SUB,0}$ on CHF in upflow

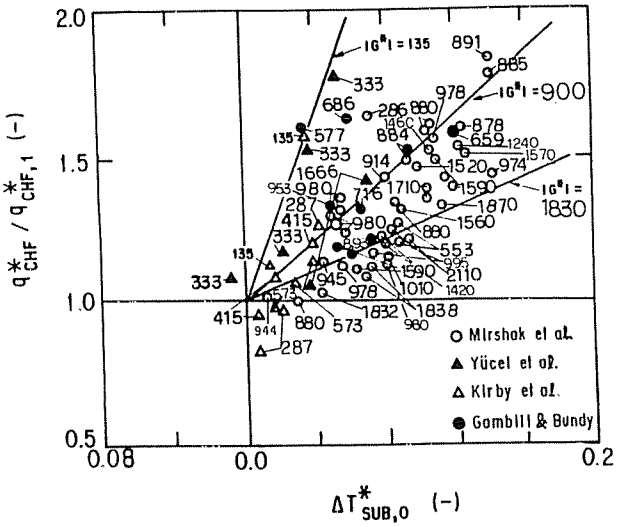

Fig. 5 Effects of $\Delta T^*_{SUB,0}$ on CHF in downflow

estimate effects of $\Delta T_{SUB,0}$, based on previously investigated results. In the region of $q^*_{CHF,1} \geq q^*_{CHF,2}$, CHF is well correlated by Eq. (1) for the saturated single phase and two-phase flow conditions, i.e., under the condition with no subcooling at the outlet of channel. Experimental conditions of the available existing CHF tests investigated in this study are listed in Table 1. The experimental data were investigated within the ranges of pressure of 0.1 to 4 MPa, mass flux of $-25{,}800$ to $+6250$ kg/m^{2}s including stagnant flow conditions, inlet subcooling of 1 to 213 K, outlet condition extending from subcooling of 0-74 K to quality of 0-1.0, and ratio of heated length to equivalent hydraulic diameter L/De of 8 to 240.

It should be mentioned here that the experimental data of Sudo et al. and Kaminaga et al. constitute 58 percent of total experimental data listed in Table 1. The estimated uncertainty of these CHF data was 3 percent based on the estimations of heat loss from the test channel and so on. Besides, the CHF data in Table 1 would be mixed with the flow excursion data because no criteria were applied for distinguishing one from the other.

The CHF experimental data for upflow and downflow are shown in Figs. 4 and 5, respectively, to make clear the effects of the outlet subcooling $\Delta T_{SUB,0}$ on the CHF, taking the ratio of $q^*_{CHF}/q^*_{CHF,1}$ as the ordinate and $Cp \cdot \Delta T_{SUB,0}/h_{fg}$ ($= \Delta T^*_{SUB,0}$), which is a dimensionless parameter for $\Delta T_{SUB,0}$, as the abscissa. These CHF experimental data were obtained in rectangular channels, except for those of Kirby et al. In the figures straight lines are illustrated to show a rough tendency on $|G^*|$. The fluid conditions of experimental data shown in Figs. 4 and 5 are subcooled at the channel outlet. It is pointed out on the

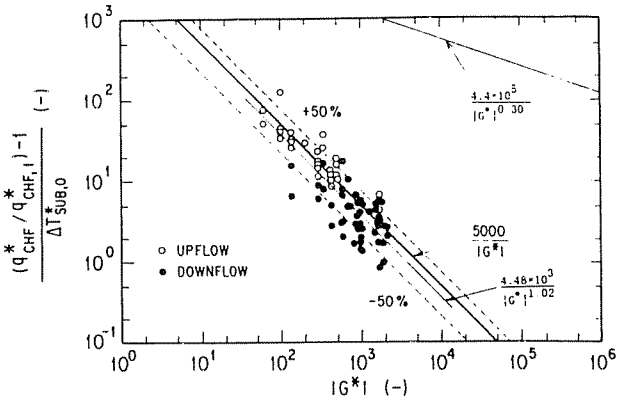

Fig. 6 Effects of $\Delta T^*_{SUB,0}$ on CHF as a function of G^* for both upflow and downflow (Gambill and Bundy, 1961; Kirby et al., 1967; Mirshak et al., 1959; Yücel and Kakac, 1978)

whole from Figs. 4 and 5 that the value of q^*_{CHF} for both upflow and downflow is greater than the values predicted by Eq. (1), and it increases with increases of $\Delta T^*_{SUB,0}$, under the same $|G^*|$ in the region of $\Delta T^*_{SUB,0}$ greater than zero, though the data scatter over a rather wide range. It is recognized in the figures that $|G^*|$ in the data for upflow is rather smaller than that for downflow at the same condition of $\Delta T^*_{SUB,0}$, but a significant and systematic tendency seems to be recognized commonly to upflow and downflow in Figs. 4 and 5: that $q^*_{CHF}/q^*_{CHF,1}$ increases with decreasing $|G^*|$ under the same $\Delta T^*_{SUB,0}$.

Figure 6 shows the data for both upflow and downflow to make clear a relationship between the effects of $\Delta T^*_{SUB,0}$ and $|G^*|$, taking $(q^*_{CHF}/q^*_{CHF,1} - 1)/\Delta T^*_{SUB,0}$ as the ordinate and $|G^*|$ as the abscissa. A bold solid line shown in Fig. 6 is a best-fit line for the data and is expressed as follows:

$$\frac{q^*_{CHF}}{q^*_{CHF,1}} = 1 + \frac{5000}{|G^*|}\Delta T^*_{SUB,0} \tag{11}$$

It should be mentioned here in Fig. 6 and in Eq. (11) that the CHF increases with an increase of $\Delta T^*_{SUB,0}$ and the effect of $\Delta T^*_{SUB,0}$ increases with a decrease of $|G^*|$. From Figs. 4 and 5, the effect of $\Delta T^*_{SUB,0}$ on q^*_{CHF} for upflow seemed to be different from that for downflow. It is now understood that it was due to the difference in the magnitude of $|G^*|$ and was not to the difference in flow direction. The CHF for both upflow and downflow can be expressed by Eq. (11) in the same way, considering the effects of both $\Delta T^*_{SUB,0}$ and $|G^*|$.

Theoretical and physical reasoning do not yet explain why the effects of $\Delta T^*_{SUB,0}$ and $|G^*|$ can be expressed in the form of Eq. (11), but the following discussion should help in understanding the reason or give us some clue for it.

Under the condition of subcooled forced-convection flow, the dimensionless heat flux q^* is expressed as below by using dimensionless heat transfer coefficient h^* and dimensionless temperatures, T^*_w and T^*_b.

$$q^* = h^*(T^*_w - T^*_b) = h^*(\Delta T^*_s + \Delta T^*_b)$$

The q^*_{CHF} under the subcooled condition can, therefore, be expressed as

$$q^*_{CHF} = h^*\Delta T^*_s\left(1 + \frac{\Delta T^*_{SUB,0}}{\Delta T^*_s}\right)$$

at the channel exit.

Here, $h^*\Delta T^*_s$ is assumed to be approximately equal to $q^*_{CHF,1}$, which is the CHF under the saturated condition, and thus,

$$\frac{(q^*_{CHF}/q^*_{CHF,1}) - 1}{\Delta T^*_{SUB,0}} = \frac{1}{\Delta T^*_s}.$$

It is well known that a form of $\Delta T^*_s = A \cdot q^{*n}$ can be applied not only in the fully developed nucleate boiling region but also in the region from the departure of nucleate boiling to the critical heat flux point.

Thom et al. (1966) reported that n is 1/2 for forced-convection nucleate boiling. On the other hand, Gaertner (1965) reported from a photographic study of nucleate pool boiling that n is 1/0.6 in the second transition region where the burnout will follow after the departure of fully developed nucleate boiling.

By using the correlation $q^*_{CHF,1} = 0.005|G^*|^{0.611}$ under the saturated conditions obtained so far, the following are introduced from the correlations proposed by Thom et al. and Gaertner, respectively:

$$\frac{(q^*_{CHF}/q^*_{CHF,1}) - 1}{\Delta T^*_{SUB,0}}\left(=\frac{1}{\Delta T^*_s}\right) = \frac{4.4\times10^5}{|G^*|^{0.30}}$$

and

$$\frac{(q^*_{CHF}/q^*_{CHF,1}) - 1}{\Delta T^*_{SUB,0}}\left(=\frac{1}{\Delta T^*_s}\right) = \frac{4.48\times10^3}{|G^*|^{1.02}}$$

These correlations are illustrated in Fig. 6 for comparison. It is very suggestive that the latter gives almost the same prediction as Eq. (11). More accumulation of experimental data on q^* versus ΔT^*_s in the region from the departure of fully developed nucleate boiling to the CHF point should, therefore, help in understanding the mechanism of critical heat flux.

It is also pointed out as one of the major features in Fig. 6 that no significant differences in the tendency of $(q^*_{CHF}/q^*_{CHF,1} - 1)/\Delta T^*_{SUB,0}$ versus $|G^*|$ are observed between upflow and downflow for $|G^*|$ larger than about 500. On the other hand, there seems to be a tendency that the values of $(q^*_{CHF}/q^*_{CHF,1} - 1)/\Delta T^*_{SUB,0}$ for downflow are smaller than those for upflow for $|G^*|$ less than 200.

It would be pointed out as a major reason for this that heat transfer will deteriorate near the heated surface because of accumulation of bubbles generated near the heated surface, due to the intensified effect of buoyancy when mass flux becomes relatively low in the subcooled downflow. The speed of bubbles rising in a stagnant water column will be 0.01 to 0.3 m/s. Bubbles will be stagnant in downflow with $|G^*|$ of 2 to 80 when bubbles are assumed to be 0.1 to 1 mm in diameter at a system pressure of 0.1 to 4 MPa, according to the experimental results of Peebles and Garber (1953). It would be, therefore, understood that there is no difference in characteristics of the CHF between upflow and downflow for $|G^*|$ larger than 500, which is significantly larger than 2-80. On the other hand, the CHF for downflow would become smaller than that for upflow when $|G^*|$ approaches 80–2.

A Modified CHF Correlation Scheme

From the discussion above, a new CHF correlation, in which the effect of subcooling at the channel outlet is considered, is proposed by using Eqs. (1) and (11), and is expressed as follows:

$$q^*_{CHF,4} = 0.005 \cdot |G^*|^{0.611}\left(1 + \frac{5000}{|G^*|}\cdot\Delta T^*_{SUB,0}\right) \tag{12}$$

Equation (12) shows that the CHF increases with an increase of $\Delta T^*_{SUB,0}$ and the effect of $\Delta T^*_{SUB,0}$ on the CHF increases with a decrease of $|G^*|$ compared with Eq. (1). Now, Eq. (12) can be applicable to both upflow and downflow in the range of $q^*_{CHF,1} \le q^*_{CHF,2}$.

Equation (12) is rewritten as follows with the subcooling at the inlet of the channel, $\Delta T^*_{SUB,in}$ ($= Cp \cdot \Delta T_{SUB,in}/h_{fg}$) because of $\Delta T^*_{SUB,0} = \Delta T^*_{SUB,in} - (q^*/G^*) \cdot (A_H/A)$:

$$q^*_{CHF,4} = 0.005 \cdot |G^*|^{0.611} \cdot \frac{1 + \frac{5000}{|G^*|}\cdot\Delta T^*_{SUB,in}}{1 + 25 \cdot |G^*|^{(-1.389)}\cdot\frac{A_H}{A}} \tag{13}$$

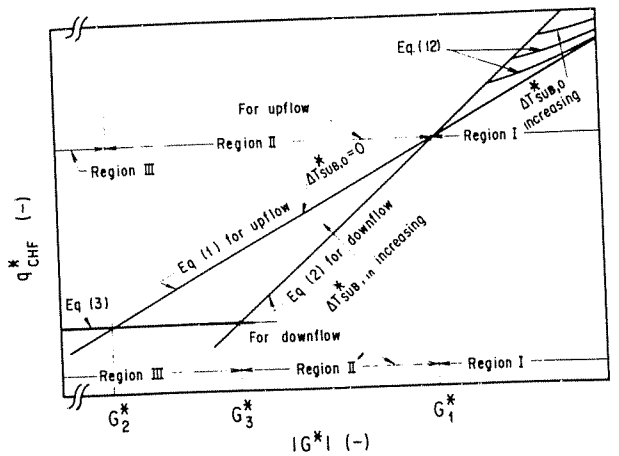

Fig. 7 Modified CHF scheme proposed in this study

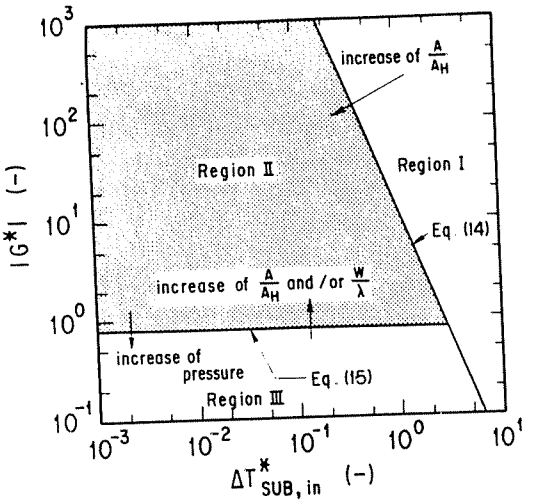

Fig. 8(a) Identification of Regions I, II, and III for upflow

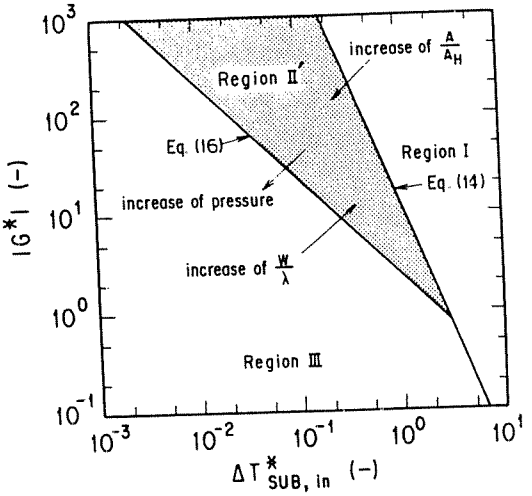

Fig. 8(b) Identification of Regions I, II', and III for downflow

It should be noted here that in the case of nonuniform heat flux channels, such as those of Kaminaga et al., Eq. (13) cannot be applied directly to the prediction of CHF. Some additional consideration, such as adoption of the maximum heat flux as the CHF, should be paid to Eq. (13), though this gives a conservative prediction of the CHF for nonuniform heat flux channels.

Thus, Fig. 7 presents the scheme of CHF correlations proposed newly in this study for upflow and downflow, taking q^*_{CHF} as the ordinate and $|G^*|$ as the abscissa. Equation (12) is a new correlation for predicting the CHF under high mass flux for both upflow and downflow. In Fig. 7, three regions for a high, medium, and low mass flux are defined as Region I. Region II, and Region III for upflow, and Region I, Region II′, and Region III for downflow.

It should be mentioned here that Eq. (2) gives the upper limits for Eq. (12) in Region I of $G^* > G^*_1$ as shown in Fig. 7 because Eq. (2) gives the condition of $\Delta T^*_{SUB,0} = 0$ for both upflow and downflow in Region I of $G^* > G^*_1$.

In Region I where the mass flux is high, a difference in CHF is not observed between upflow and downflow in this study and the CHF for both upflow and downflow is well predicted by Eq. (12). In this region, $\Delta T^*_{SUB,0}$ and G^* have significant effects on the CHF. A larger $\Delta T^*_{SUB,0}$ gives a larger CHF with the same $|G^*|$ and a larger $|G^*|$ gives a larger CHF with the same $\Delta T^*_{SUB,0}$.

In the medium mass flux region, the CHF for downflow is expressed by Eq. (2) and is much lower than that for upflow with the same $|G^*|$. Therefore, a flow direction has a significant effect on the CHF in the medium mass flux region. In Region II for upflow where $\Delta T^*_{SUB,0} = 0$, the CHF is predicted solely by Eq. (1) and only G^* has a significant effect on the CHF. On the other hand, in Region II′ for downflow, the CHF is predicted by Eq. (2). In this region, $\Delta T^*_{SUB,in}$, $|G^*|$ and a ratio of the flow area to the heated area, A/A_H, have significant effects on CHF.

In Region III for both upflow and downflow where mass flux is very low or the flow condition is a countercurrent flow with $G^* = 0$, CHF is predicted by Eq. (3). In this region, the ratio of the flow area to the heated area, A/A_H, and a channel width W have significant effects on the CHF. Under the CCFL condition with a large L/De the temperature of water supplied into the channel would at last become a saturated temperature because water is well mixed with upflowing steam generated in the channel at the top of the channel, even if water is subcooled at first. Therefore, $\Delta T^*_{SUB,in}$ and $|G^*|$ would have no significant effects on the CHF. Equation (3) is a common correlation for predicting the minimum CHF for both upflow and downflow.

Figures 8(*a*) and 8(*b*) illustrate the regions described above for upflow and downflow, respectively, taking $|G^*|$ as the ordinate and $\Delta T^*_{SUB,in}$ as the abscissa. These regions are functions of not only $|G^*|$ but also $\Delta T^*_{SUB,in}$.

A boundary between Region I and Region II or II′ is calculated and identified as follows by using Eqs. (1) and (2):

$$G^*_1 = \left(\frac{0.005}{\frac{A}{A_H} \Delta T^*_{SUB,in}} \right)^{\frac{1}{0.389}} \tag{14}$$

Equation (14) shows that G^*_1 decreases with an increase of $\Delta T^*_{SUB,in}$ and a larger A/A_H gives a smaller G^*_1 with the same $\Delta T^*_{SUB,in}$.

A boundary between Region II and Region III is calculated and identified as follows by using Eqs. (1) and (3):

$$G^*_2 = \left[140 \cdot \frac{A}{A_H} \cdot \frac{\sqrt{W/\lambda}}{\left\{ 1 + \left(\frac{\rho_g}{\rho_l} \right)^{1/4} \right\}^2} \right]^{\frac{1}{0.611}} \tag{15}$$

Equation (15) shows that G^*_2 increases with an increase of A/A_H and W/λ. With increasing pressure, ρ_g/ρ_l would increase; therefore, G^*_2 would decrease. Equation (15) is not a function of $\Delta T^*_{SUB,in}$.

A boundary between Region II′ and Region III is calculated and identified as follows by using Eqs. (2) and (3):

$$G_3^* = 0.7 \cdot \frac{\sqrt{W/\lambda}}{\left\{1 + \left(\frac{\rho_g}{\rho_l}\right)^{1/4}\right\}^2} \cdot \Delta T^*_{SUB,in} \quad (16)$$

Equation (16) shows that G_3^* increases with an increase of W/λ and decreases with an increase of $\Delta T^*_{SUB,in}$. With increasing pressure, ρ_g/ρ_l would increase, and therefore, G_3^* would decrease.

Comparison of Modified CHF Correlation Scheme and Experimental Data

Figures 9(*a–d*) show the comparisons of all the available experimental data shown in Table 1 with the modified CHF scheme, taking the measured q^*_{CHF} as the ordinate and q^*_{CHF} predicted by the CHF scheme as the abscissa, in order to estimate the error of the CHF scheme. The figures on the right-hand side show the region where the data belong, taking $|G^*|$ as the ordinate and $\Delta T^*_{SUB,in}$ as the abscissa.

Figure 9(*a*) shows the comparison of all the experimental data that belong to Region I for both upflow and downflow with Eq. (12), $q^*_{CHF,4}$. Region I is identified by using Eq. (14). The comparison shows that Eq. (12) gives a good prediction, allowing the rms error of ±33 percent to the lower and upper limits of the experimental data.

Figure 9(*b*) shows the comparison of all the experimental data that belong to Region II for upflow with Eq. (1), $q^*_{CHF,1}$. Region II is identified by using the combination of Eqs. (14) and (15). The comparison shows that Eq. (1) gives a good prediction, allowing the rms error of −33 percent as the lower limit of the experimental data. In this region some of the data are greater than +33 percent of the values predicted by Eq. (1).

Figure 9(*c*) shows the comparison of all the experimental data that belong to Region II′ for downflow with Eq. (2), $q^*_{CHF,2}$. Region II′ is identified by using the combination of Eqs. (14) and (16). The comparison shows that Eq. (2) gives a good prediction, allowing the rms error of −33 percent as the lower limit of the experimental data. In this region some of the data show the errors greater than +33 percent to the values predicted by Eq. (2).

Figure 9(*d*) shows the comparison of all the experimental data that belong to Region III for both upflow and downflow with Eq. (3), $q^*_{CHF,3}$. Region III is identified by using Eq. (15) for upflow and Eq. (16) for downflow. The comparison shows that Eq. (3) gives a good prediction, allowing the rms error of −33 percent as the lower limit of the experimental data. In this region some of the data also show rms errors greater than +33 percent for the values predicted by Eq. (3).

Figures 10(*a*, *b*, *c*) show comparisons of the Zenkevich, Katto, and Gambill correlations, which can evaluate the effects of mass flux and subcooling with experimental data for Region I in both upflow and downflow, respectively. The predictions from the correlations are not as good as that from Eq. (12).

Comparison of the results of all the experimental data with

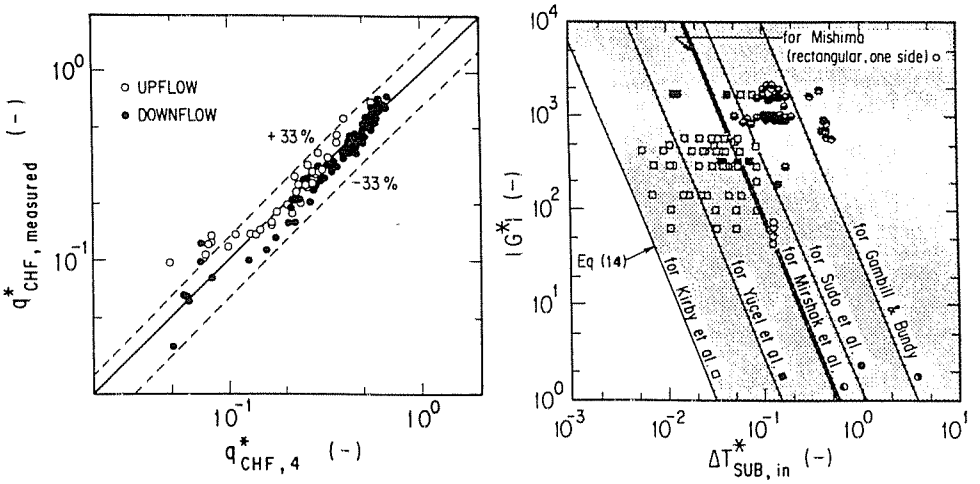

Fig. 9(*a*) Comparison of CHF between prediction (Eq. (12)) and the experimental results (Gambill and Bundy, 1961; Kirby et al., 1967; Mirshak et al., 1959; Mishima, 1984; Sudo et al., 1985a; Yücel and Kakac, 1978) for Region I in both upflow and downflow

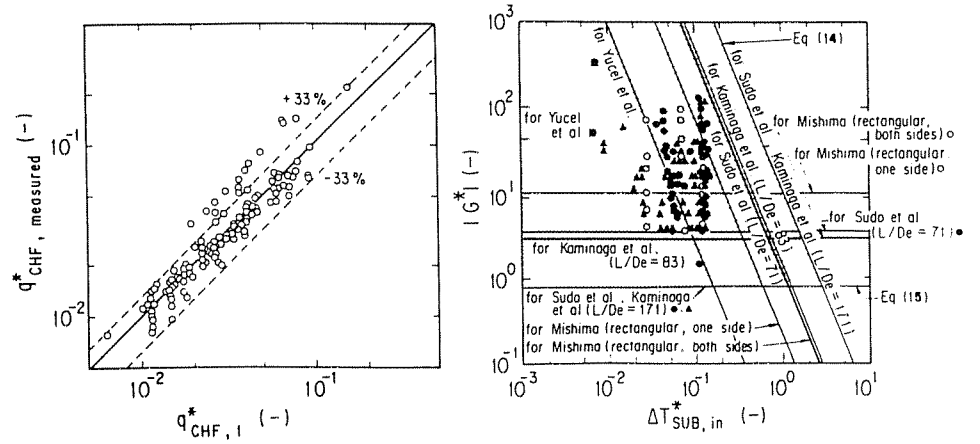

Fig. 9(*b*) Comparison of CHF between prediction (Eq. (1)) and experimental results (Kaminaga et al., 1991; Mishima, 1984; Sudo et al., 1985a; Yücel and Kakac, 1978) for Region II in upflow

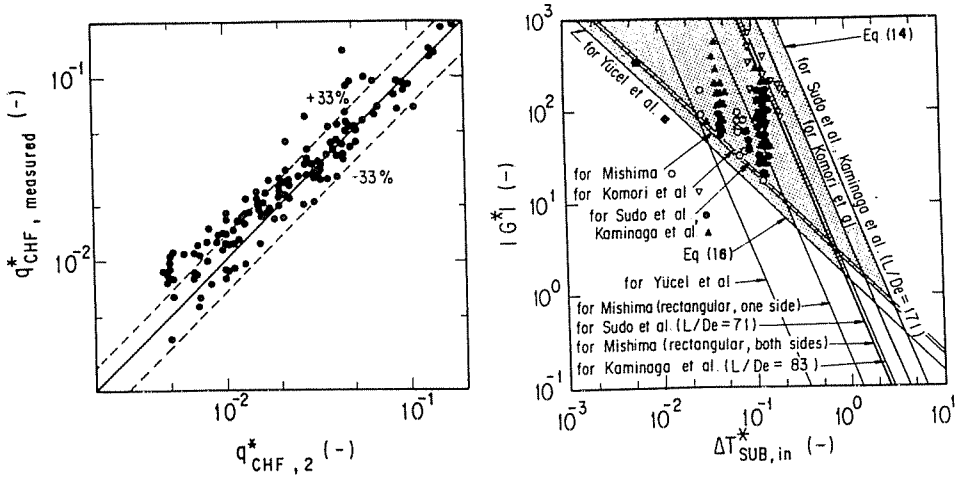

Fig. 9(c) Comparison of CHF between prediction (Eq. (2)) and the experimental results (Kaminaga et al., 1991; Komori et al., 1990; Mishima, 1984; Sudo et al., 1985a; Yücel and Kakac, 1978) for Region II′ in downflow

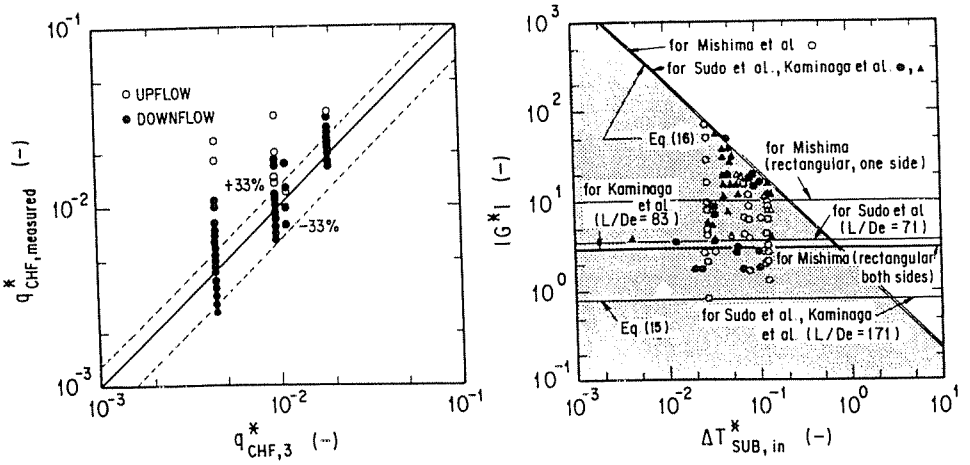

Fig. 9(d) Comparison of CHF between prediction (Eq. (3)) and the experimental results (Kaminaga et al., 1991; Mishima, 1984; Sudo et al., 1985a) for Region III in both upflow and downflow

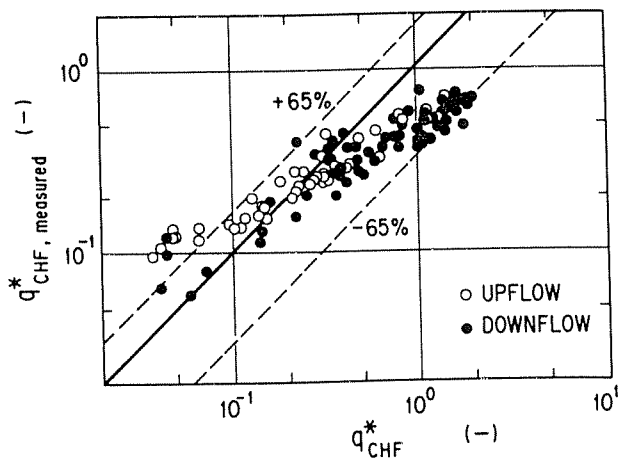

Fig. 10(a) Comparison of Zenkevich correlation (Eq. (9)) with experimental data for Region I in both upflow and downflow (Gambill and Bundy, 1961; Kirby et al., 1967; Mirshak et al., 1959; Mishima, 1984; Sudo et al., 1985a; Yücel and Kakac, 1978)

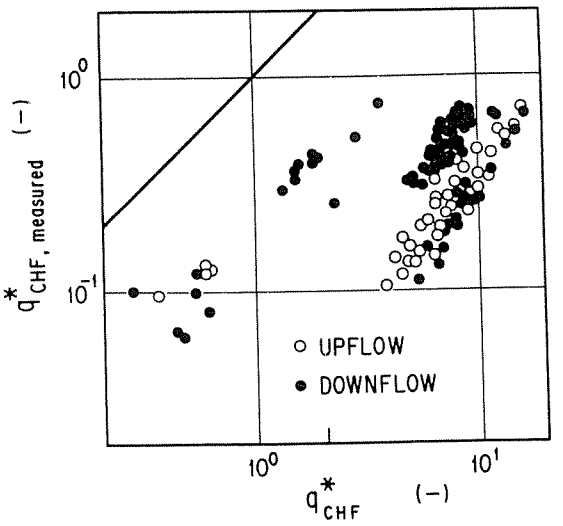

Fig. 10(b) Comparison of Katto correlations (Eqs. (4)-(6)) with experimental data for Region I in both upflow and downflow (Gambill and Bundy, 1961; Kirby et al., 1967; Mirshak et al., 1959; Mishima, 1984; Sudo et al., 1985a; Yücel and Kakac, 1978)

the modified CHF scheme described above show that Eqs. (1), (2), (3), and (12) give good predictions against almost all the experimental data. But Eqs. (1), (2), and (3) somewhat underpredict the CHF against some of the experimental data even though the rms errors of 33 percent are allowed. It is considered that these errors are due to the following reasons: (1) The experimental data were obtained under various experimental conditions (pressure, configuration of channels, etc.) as shown in Table 1, but the predicted CHF for each of Regions I, II, II′, and III was calculated by only one correlation, which was

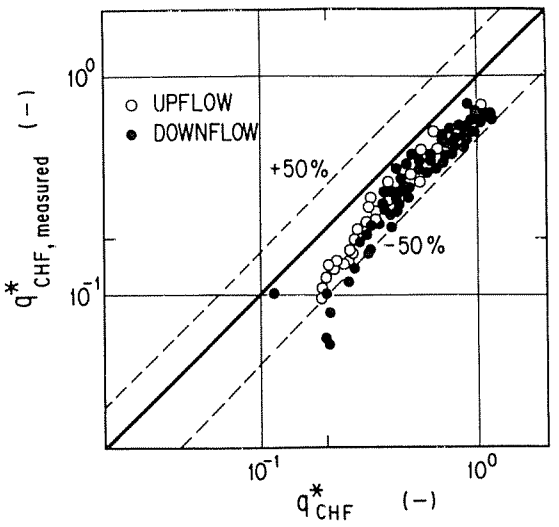

Fig. 10(c) Comparison of the correlation of Gambill et al. (Eq. (10)) with experimental data for Region I in both upflow and downflow (Gambill and Bundy, 1961; Kirby et al., 1967; Mirshak et al., 1959; Mishima, 1984; Sudo et al., 1985a; Yücel and Kakac, 1978)

proposed by the authors. (2) For Region III, the experimental data themselves scattered widely because the flow in this region was not stable due to low flow rates. (3) For Region II′, the experimental data themselves also scattered widely, even though flow rate in this region was greater than that in Region III, because the flow was not stable under the condition of cocurrent downflow or countercurrent flow.

From the viewpoint of thermohydraulic design and safety evaluation of the nuclear research reactors, however, it is considered that these underpredictions are the margin for using these correlations. As the rms error of −33 percent is estimated for the CHF scheme, it is recommended that the Minimum DNB (Departure from Nucleate Boiling) Ratio should be larger than 1.5, which is equivalent to an rms error of −33 percent in this study, in the case that the proposed CHF scheme is adopted in the core thermohydraulic design.

Conclusions

This study investigated the kind of factors that affect CHF, and it was found that mass flux, inlet subcooling, outlet subcooling, flow direction, pressure, and configuration of channels have significant effects on CHF. The effects of these factors on CHF were also estimated. A CHF scheme for both upward and downward flows was, thus, established within the ranges of pressure of 0.1 to 4 MPa, mass flux of −25,800 to +6250 kg/m^{2}s including stagnant flow conditions, inlet subcooling of 1 to 213 K, outlet condition extending from subcooling of 0–74 K to quality of 0–1.0, and the ratio of heated length to equivalent hydraulic diameter L/De of 8 to 240. It was also made clear that rms errors of CHF correlations used in the proposed CHF scheme were within −33 percent. It is proposed that when this CHF scheme is applied, the Minimum DNB Ratio should be larger than 1.5, which is equivalent to the correlation error of −33 percent, in the core thermohydraulic design of nuclear research reactors.

References

Gaertner, R. F., 1965, "Photographic Study of Nucleate Pool Boiling on a Horizontal Surface," ASME JOURNAL OF HEAT TRANSFER, Vol. 87, pp. 17–29.

Gambill, W. R., and Bundy, R. D., 1961, "HFIR Heat Transfer Studies of Turbulent Water Flow in Thin Rectangular Channels," ORNL-3079.

Hirano, M., and Sudo, Y., 1986, "Analytical Study on Thermal-Hydraulic Behavior of Transient From Forced Circulation to Natural Circulation in JRR-3," *J. Nucl. Sci. Technol.*, Vol. 23(4), pp. 352–368.

Kaminaga, M., Sudo, Y., Usui, T., and Murayama, Y., 1991, "Experimental Study of Critical Heat Flux in a Narrow Vertical Rectangular Channel," *Heat Transfer—Japanese Research*, Vol. 20(1), pp. 72–85.

Katto, Y., 1981, "Dimensionless Critical Heat Flux of Forced Convection Boiling in Uniformly Heated Rectangular Channel," *JSME, B*, Vol. 47[424], pp. 2351–2357 [in Japanese].

Kirby, G. J., Stanforth, R., and Kinneir, J. H., 1967, "A Visual Study of Forced Convection Boiling, Part 2, Flow Patterns and Burnout for a Round Tube Test Section," AEEW-R506.

Komori, Y., Kaminaga, M., Sakurai, F., Ando, H., Nakata, H., Sudo, Y., and Futamura, Y., 1990, "Experimental Study on DNB Heat Flux Correlations for JMTR Safety Analysis," presented at the Int. Mtg. on Reduced Enrichment for Research and Test Reactors, Newport, RI, Sept. 23–27.

Mirshak, S., Durant, W. S., and Towell, R. H., 1959, "Heat Flux at Burnout," DP-355, U.S.AEC.

Mishima, K., et al., 1983, "CHF Correlation Related to the Core Cooling of a Research Reactor," *Proc. Int. Mtg. on Reduced Enrichment for Research and Test Reactors*, Tokai, Japan, Oct. 24–27, pp. 311–320.

Mishima, K., 1984, "Boiling Burnout at Low Flow Rate and Low Pressure Conditions," Dissertation Thesis, Kyoto University, Japan.

Peebles, F. N., and Garber, H. J., 1953, "Studies on the Motion of Gas Bubbles in Liquids," *Chem. Eng. Prog.*, Vol. 49-2, pp. 88–97.

Siman-Tov, M., Gambill, W. R., Nelson, W. R., Ruggles, A. E., and Yoder, G. L., 1991, "Thermal-Hydraulic Correlations for the Advanced Neutron Source Reactor Fuel Element Design and Analysis," presented at the ASME Winter Annual Meeting, Atlanta, GA, Dec. 1–6.

Sudo, Y., Miyata, K., Ikawa, H., Kaminaga, M., and Ohkawara, M., 1985a, "Experimental Study of Differences in DNB Heat Flux Between Upflow and Downflow in Vertical Rectangular Channel," *J. Nucl. Sci. Technol.*, Vol. 22(8), pp. 604–618.

Sudo, Y., Ando, H., Ikawa, H., and Ohnishi, N., 1985b, "Core Thermodynamic Design With 20% LEU Fuel for Upgraded Research Reactor JRR-3," *J. Nucl. Sci. Technol.*, Vol. 22(7), pp. 551–563.

Thom, J. R. S., Walker, W. M., Fallon, T. A., and Reising, G. F. S., 1966, "Boiling in Sub-cooled Water During Flow up Heated Tubes or Annuli," *Proc. Inst. Mech. Engrs.*, Vol. 180, Pt. 3C, pp. 226–246.

Yücel, B., and Kakac, S., 1978, "Forced Flow Boiling and Burnout in Rectangular Channels," *Proc. 6th Int. Heat Transfer Conf.*, Vol. 1, pp. 387–392.

Zenkevich, B. A., 1959, "The Generalization of Experimental Data on Critical Heat Fluxes in Forced Convection of Sub-cooled Water," *J. Nucl. Energy, Part B: Reactor Technology*, Vol. 1, pp. 130–133.